A 3 – 18 GHz UWB Antenna with modified feed-line

Srikanth Itapu (sitapu@rockets.utoledo.edu)
University of Toledo https://orcid.org/0000-0002-6394-0003

Short Report

Keywords: CPW feed, Microstrip feed, Modified ground plane, Monopole Antenna

Posted Date: March 24th, 2021

DOI: https://doi.org/10.21203/rs.3.rs-173254/v1

Abstract

A Co-Planar Waveguide fed circular ultra-wide band antenna with modified ground-plane and feedline is designed on a FR4 (ϵ_r=4.3) substrate of thickness $0.01\lambda_0$. The proposed antenna exhibits an overall impedance bandwidth ranging from 2.99 GHz to 18.0 GHz and beyond (with S_{11}< -10 dB). Design parameters have been optimized to achieve the UWB bandwidth. The measured radiation patterns of this antenna are omnidirectional in H- plane and bidirectional in E-plane. An extended impedance bandwidth is achieved as a result of modified feed-line. The proposed antenna can be used for medical imaging and urban IoT applications.

1. Introduction

The Federal Communications Commission (FCC) had envisaged as early as in the year 2002 that Ultra-wideband (UWB) communication systems offers salient features such as low-power, higher data rates, ubiquitous connectivity, etc. [1]. Printed antennas are preferred over conventional ones for such application-specific systems due to their conformity, compact size, and integration in microwave circuits [2]. To further enhance the performance of UWB systems, compact antenna with Co-planar Waveguide (CPW) feeds, are preferred over other feeding mechanisms (Slot-line, Microstrip line, etc.) which offer advantages, such as wider bandwidths, lower radiation loss, and dispersion [3-4].

Several CPW-fed UWB antenna designs have been reported previously, which differ by factors such as the shape of the radiating element, notch characteristics and configuration of the ground plane. The antenna design in [5] is based on circular disc radiating element with partial rectangular ground plane. The authors in [6] report on a step-typed monopole antenna with a tapered-step ground plane. One of the most commonly designed antenna in literature is the crescent shaped element [7] where the antenna consists of an open annulus strip as a ground plane and a semi-circular crescent with multiple cuts in [8]. The authors of [9] introduced annular slot and round corners into the ground and use a round-edged bowtie-shaped conductor. All the UWB antennas presented satisfy the requirement of FCC band [10-16]. In [17], a circular monopole antenna with tapered feed-line but ground plane on the back side of the radiating element was proposed, which was compact in size and exhibited a bandwidth ranging from 6.5 GHz to 25 GHz. In [18] again, a circular monopole antenna was proposed with modified ground plane at the back-end and a minimal feedline. The design was complex and in interpreting the ground plane and offered bandwidth of about 7 GHz. In [19], a hemispherical monopole with ground plane at the back-end was proposed offering a frequency range of 2.8 to 11.97 GHz and an elliptic patch antenna was discussed as a body-coupled wideband antenna with close to 4 GHz bandwidth in [20]. A circular monopole antenna with a pentagonal cut on the radiating element and ground plane on the back-end exhibited a huge bandwidth from 4 GHz to 40 GHz in [21]. Therefore, there is a need to design antennas which can support future UWB systems with wider bandwidths, without compromising on the ground plane and feedline.

In this paper, the antenna structure proposed is an extended circular monopole design. The proposed structure and the modified rectangular ground plane together provide a wide impedance bandwidth from

2.99 to 18.0 GHz. This compact antenna is of size (length x breadth x height) $0.5\lambda_0$ x $0.4\lambda_0$ x 0.01 λ_0 and is discussed in terms of the impedance bandwidth, current distributions, radiation patterns and peak gain in the following sections. Section 2 presents the antenna design with iterations as well as comparison of simulated and measured impedance bandwidths. Section 3 deals with the optimization of design parameters in order to achieve the requisite enhancements in bandwidth and finally the radiation patterns, peak gain and radiation efficiency are presented.

2. Circular Monopole Antenna With Modified Ground And Feed Design

Figure 1 depicts the circular UWB antenna with modified feed and ground plane. In the design, the radiating element is a copper-plated circle patch with a radius 11mm on a FR4 dielectric substrate (ε_r = 4.3). The 50Ω feedline is modified in order to provide better impedance matching. There is a 0.5mm separation between the feedline and the ground plane and 0.6mm between radiating element and the ground plane. Table 1 accentuates the imminent need to optimize the design as compared to the previously published reports available in the literature.

Table 1. Comparison of other relevant published works.

Ref.	Radiating element size (λ_0 at center frequency)	Frequency range (bandwidth)	Comments
[16]	$0.83\lambda_0$ x $0.6\lambda_0$ x $0.04\lambda_0$	6.25 GHz to 25 GHz (18.75 GHz)	Tapered feed-line but ground on the back side of the radiating patch.
[17]	$0.86\lambda_0$ x $1.19\lambda_0$ x $0.034\lambda_0$	3 GHz to 10 GHz (7 GHz)	Very short feed-line with partial complex-structured ground plane on the back side of the radiating patch.
[18]	$0.89\lambda_0$ x $0.78\lambda_0$ x $0.019\lambda_0$	2.8 GHz to 11.97 GHz (9.17 GHz)	Hemispherical radiating patch with ground plane on the back side of the radiating patch.
[19]	$0.2\lambda_0$ x $0.3\lambda_0$ x $0.05\lambda_0$	2.5 GHz to 5 GHz (2.5 GHz)	An elliptical radiating patch with modified ground plane and very high dielectric substrate.
[20]	$2.066\lambda_0$ x $1.25\lambda_0$ x $0.102\lambda_0$	4 GHz to 40 GHz (36 GHz)	Circular monopole with pentagonal cut and rectangular cut on the feed-line with ground plane on the back side of the radiating patch.
This work	$1.4\lambda_0$ x $1.75\lambda_0$ x $0.025\lambda_0$	3 GHz to 18 GHz (15 GHz)	With a slight increase in the dimensions and co-planar configuration, the large impedance bandwidth is achived.

The dimensions of the substrate are 50mm x 40mm with co-planar feeds as two rectangular ground patches with bent edges near the feedline and at the edges. Figure 2 depicts the iterations taken into

consideration while designing. The ground patch dimensions are optimized to 25.2mm x 17.9mm. This design provides full UWB bandwidth with an extended bandwidth up to 18GHz with VSWR < 2 (Figure 3).

3. Critical Parameters Of The Design

The width of the antenna determines the extent of current flow within the antenna as seen in the current distribution plots below (Figure 4 (a, b, c)). The current is maximum along the feedline and the ground plane adjacent to the feedline. Hence, more the width of the ground plane, the current distribution will reduce gradually till it reaches the edges. So, the width of the antenna is always optimized for maximum current distribution. The width of the feedline also is an important parameter which needs to be optimized for an optimum antenna design. As the feedline width increases, the current accumulation becomes more along the feedline and hence, current distribution in the ground becomes insignificant. Basically, the power handling capacity of the feedline increase as the width decreases. So, it is always preferable to have a minimal feedline width. The gap between the ground plane and the feedline and the gap between the radiating patch and the ground also play a major role in antenna design. Increase in the respective lengths result in reduction in the radiated power as can be observed in the radiation patterns. From the current distribution plots in Figure 4(a, b, c), it can be observed that as the frequency increases, the current distribution along the feedline is decreased and spread to the radiating patch. i.e. the current gets distributed as the frequency increases.

The proposed antenna has been optimized with respect to the ground length, ground width, gap between ground and feed and finally, the radius of the patch. To improve the gain of the antenna, the ground is truncated at the edges. The antenna is been simulated in 3D electromagnetic simulator software HFSS [22].

A. Optimization of the ground length (l_g = 25.2mm)

From Figure 5, it can be observed that the variation in the ground length from 24.8mm to 25.4mm results in a slight shift in the resonant frequency in the lower end for a value of 24.8mm. As the length is increased, there is negligible shift in the first resonant frequency. The optimization is limited to 25.4mm because the radiating patch and ground plane overlap each other for larger values. For the optimized values of l_g =25.2mm, the harmonics converge in a neat manner.

B. Optimization of the distance between ground plane and feed-line (d_{gf} = 0.5mm)

The distance between the feed and the ground is varied from 0.3mm to 0.6mm considering the feedline width to vary from 2.8mm to 3.4mm as shown in Fig. 6. The first resonant frequency shifts towards lower frequency side is observed when the feedline/ground-plane gap increases. The gap is optimized to d_{gf} =0.5mm between feedline and ground plane for which the resonant frequencies converge to provide UWB characteristics.

C. Ground plane optimization (g_p = 18mm)

The ground plane is generally considered to be in rectangular shape which results in harmonic generation. In order to reduce the harmonics, the ground is modified by bending the sharp edges to provide smooth current path to flow in the ground. Hence, the ground is curved at the edges nearer to the radiating patch. The radius of the curve is optimized for values ranging from 16mm to 19mm. The phenomenon observed in Fig.7 was no shift in the first resonant frequency. Except for the optimized value of g_p = 18mm, the return loss rises slightly above -10dB in the frequency range of 4 GHz to 5GHz which suggests impedance mismatch. Increasing the radius to 19mm results in a total impedance mismatch in the higher frequency region.

D. Optimization of the radiating patch (r = 11mm)

The radius (r) of the radiating patch is varied from 10.5mm to 11.5mm keeping the ground plane length at its optimized value 25.2mm. The results from Fig. 8 show that, for radius of 10.5mm, there is an impedance mismatch in the frequency range 7GHz to 8GHz. For r = 11.5mm, there is an impedance mismatch for frequencies between 4GHz to 5GHz. The UWB characteristic is observed for the radius of 11mm.

E. Radiating patterns

The radiation patterns of this antenna have been measured at selective frequencies. The radiation patterns were measured in anechoic chamber. The simulated and measured radiation patterns in H-plane are shown in Figure 9 and Figure 10 respectively at frequencies 3.9 GHz, 5.025 GHz, 6.15 GHz, 8.025 GHz, 10.32 GHz, 13.5 GHz and 17.02 GHz respectively. The nature of measured radiation pattern in H-plane is nearly omni-directional. Similarly, simulated and measured radiation patterns in E-plane are also measured at frequencies i.e. 5.7 GHz, 7.5 GHz, 8.35 GHz, 11.85 GHz and 16.08 GHz respectively as shown in Figure 11 and Figure 12 respectively. The nature of radiation patterns in E-plane are nearly bidirectional. It is also observed that the radiation patterns are marginally varied. It may be due to FR4 lossy substrate and edge reflection.

F. Peak gain and radiation efficiency

The peak gain of this antenna has also been simulated as shown in Figure 13. It is noticed, as the frequency increases, the gain increases. This is because, at higher frequencies, the Receiving area becomes more in comparison to short wavelength. The gain at 3GHz is 1.5dB and 10GHz it is 10.5dB. Beyond this, as the frequency increases, the gain more or less remains the same. A plausible reason could be attributed to the loss tangent of the substrate and increase in cross polarization at higher frequencies. The radiation efficiency (RE) is also simulated over the UWB frequency range (Fig. 11). The RE is 96% at 3 GHz, 90% at 7GHz and 85% at 12 GHz. A decrease in RE is observed as w.r.t frequency which can be attributed to the substrate loss tangent.

4. Conclusion

A compact UWB antenna with CPW feed has been designed and demonstrated as having a bandwidth in the range of 2.99 GHz to 18 GHz. Several designs have been investigated for an optimal design and finally a circular monopole antenna with modified ground and feedline respectively, is presented. The radiation patterns exhibit omni-directionality in E-plane and bi-directionality in H-plane. Because of its extended impedance bandwidth, the modified feed circular antenna can be used for future IoT, Vehicle-to-Vehicle technologies.

Declarations

Funding: No funding.

Conflict of Interest/Competing Interest: The author declares no conflict of interest.

Availability of data and material: Not Applicable.

Code availability: Not Applicable.

Author's Contributions: Conceptualization, Data collection, Analysis, Interpretation, Manuscript preparation, Writing and Proof-Reading.

References

1. Federal Communications Commission, *First report and order in the matter of revision of part 15 of the commission's rules regarding ultra-wideband transmission systems, ET Docket 98–153, FCC 02–48*, released April 22, 2002.
2. Balanis, C.A. (2005). *Antenna Theory, Analysis and Design.*, Hoboken, NJ, USA: Wiley.
3. Chang, D.C., Zeng, B.H. and Liu, J.C. (2008). CPW- fed circular fractal slot antenna design for dual-band applications, *IEEE Transactions on Antennas and Propagation*, 56 (12), 3630- 3636.
4. Bhobe, A.U., Holloway, C.L., Piket-May, M. and Hall, R. (2004). Wide-band slot antennas with CPW feed lines: hybrid and log-periodic designs, *IEEE Transactions on Antennas and Propagation*, 52(10), 2545-2554.
5. Liang, J., Guo, L., Chiau, C.C., Chen, X. and Parini, C.G. (2005). Study of CPW-fed circular disk monopole antenna for ultra-wideband applications, *IEE Proceedings - Microwaves, Antennas and Propagation,* 152(6), 520-526.
6. Jan, J.Y., Kao, J.C., Cheng, Y.T., Chen, W.S. and Chen, H.M. (2006). CPW-fed wideband printed planar monopole antenna for ultra-wideband operation, *IEEE Antenna and Propagation Society International Symposium* (Albuquerque, NM, U.S.A), pp. 1697-1700.
7. Chen, M.E. and Wang, J.H. (2008). CPW-fed crescent patch antenna for UWB applications, *Electronics Letters*, 44(10), 613-615.
8. Itapu, S. (2019). Semicircular slotted monopole antenna for future ultra-wideband applications*, CVR Journal of Science and Technology*, 17(1), 44-48.

9. Zhao, L., Ruan, C.L. and Qu, S.W. (2006). A novel broadband slot antenna fed by CPW, *IEEE Antennas and Propagation International Symposium* (Albuquerque, NM, U.S.A.), 2583-2586.
10. Srikanth, I. and Kumar, Raj. (2012). Fractal antenna aims at 2.9 GHz to 14.6 GHz, *Microwaves & RF*, 51(8), 69-75.
11. Kumar, Raj and Srikanth, I. (2012). Design of apollonian gasket ultrawideband antenna with modified plane, *Microwave and Optical Technology Letters*, 54(8), 1793-1796.
12. Tripathi, S., Mohan, A. and Yadav, S. (2015). A Compact Koch Fractal UWB MIMO Antenna with WLAN Band-Rejection, *IEEE Transactions on Antennas and Propagation*, 14, 1565-68.
13. Amini, A., Oraizi, H. and Zadeh, M.A.C. (2015). Miniaturized UWB Log-Periodic Square Fractal Antenna, *IEEE Transactions on Antennas and Propagation*, 14, 1322-25.
14. Ali, T., Subhash, B.K. and Biradar, R.C. (2018). A Miniaturized Decagonal Sierpinski UWB Fractal Antenna, *Progress In Electromagnetics Research C*, 84, 161-174.
15. Kumar, R., Chaubey, P.N. and Srikant, I. (2012). On the design of UWB circular fractal antenna with notched-band characteristics using W-slot, *Journal of Microwaves, Optoelectronics and Electromagnetic Applications*, 11(2), 230-241.
16. Itapu, S., Almalkawi, M. and Devabhaktuni, V. (2015). A 0.8-8 GHz multi-section coupled line balun, *Electronics*, 4(2), 274-282
17. Singha, R., Vakula, D. and Sarma, N.V.S.N. (2014). Compact concentric ring shaped antenna for ultra wide band applications, *IOP Conference Series: Materials Science and Engineering*, 67,
18. Celik, A.R. and Kurt, M.B. (2018). Development of an ultra-wideband, stable and high-directive monopole disc antenna for radar-based microwave imaging of breast cancer,*Journal of Microwave Power and Electromagnetic Energy*, 52(2), 75-93.
19. Ahmad, W., Tarczynski, A. and Budimir, D. (2017). Design of monopole antennas for UWB applications, *IEEE International Symposium on Antennas and Propagation & USNC/URSI National Radio Science Meeting* (San Diego, CA, U.S.A.).
20. Kjelgard, K.G., Hovin, M. and Lande, Tor S. (2015). Body-coupled, wideband antennas*, IEEE Biomedical Circuits and Systems Conference (BioCAS)* (Atlanta, GA, U.S.A.).
21. Saha, T.K., Goodbody, C., Karacolak, T. and Sekhar, P.K. (2019). A compact monopole antenna for ultra-wideband applications, *Microwave and Optical Technology Letters*, 61, 182-186.
22. *Ansys HFSS*, Pittsburgh, PA, 2018.

Figures

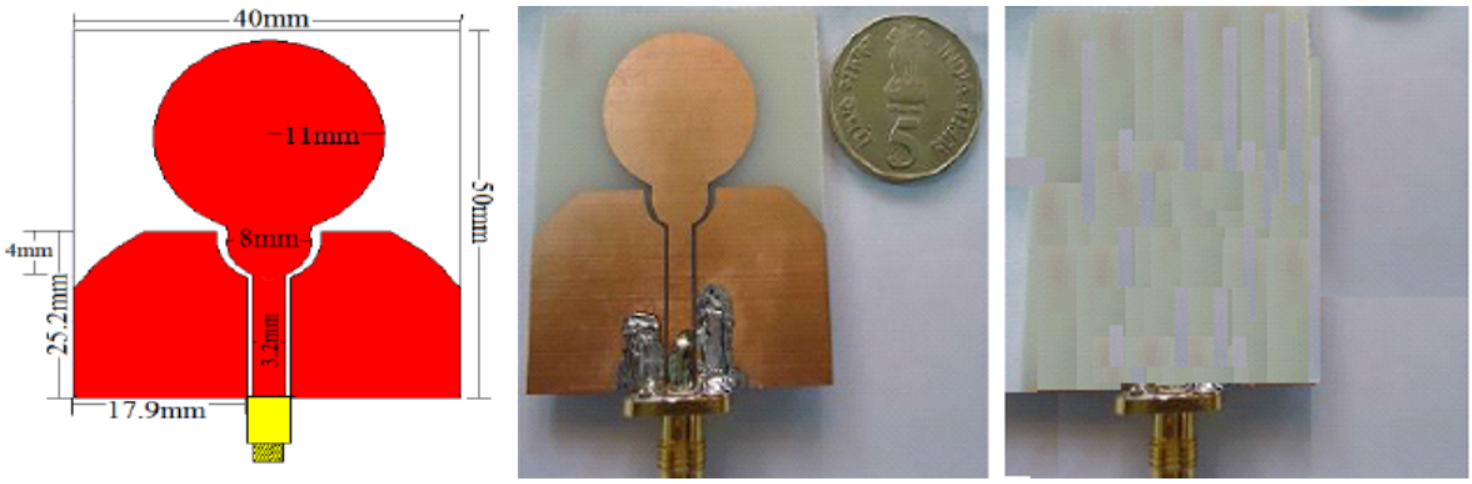

Figure 1

(a) Schematic of the proposed antenna, (b) fabricated antenna (front view), (c) antenna back view.

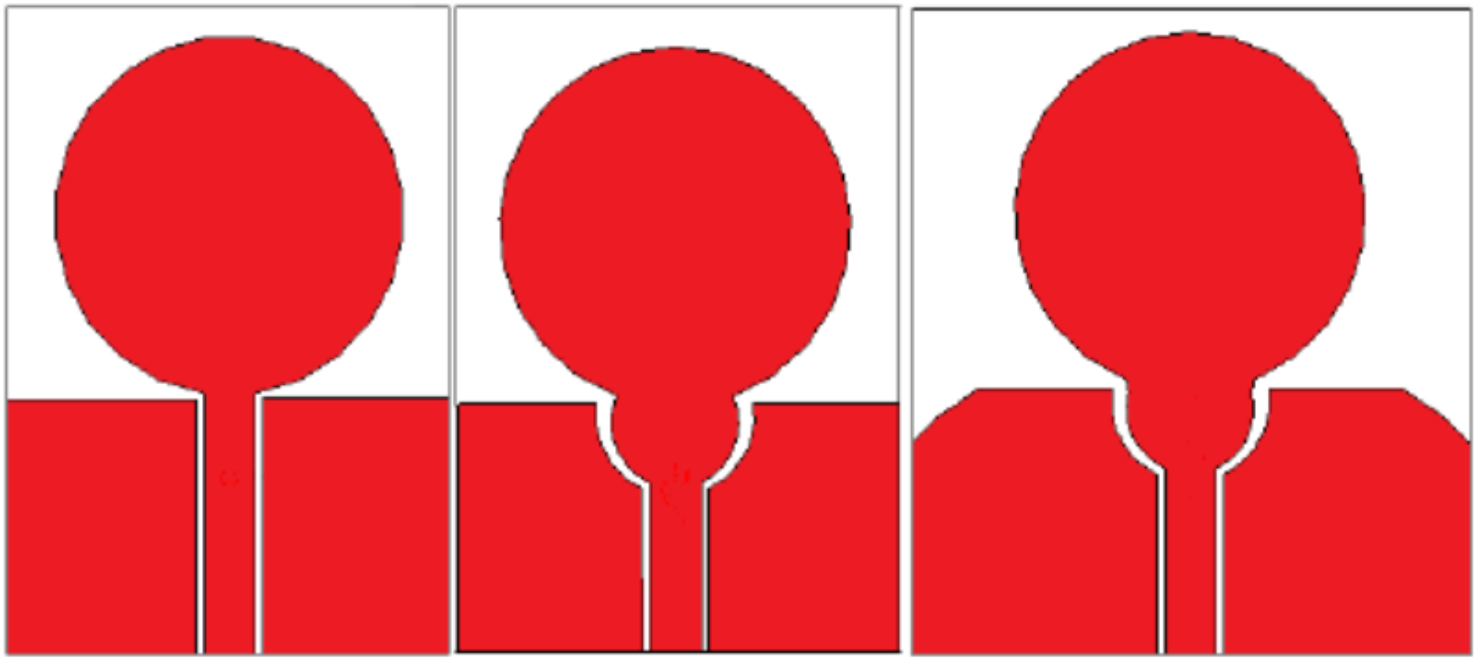

Figure 2

(a) Zeroth iteration, (b) first iteration and (c) final antenna

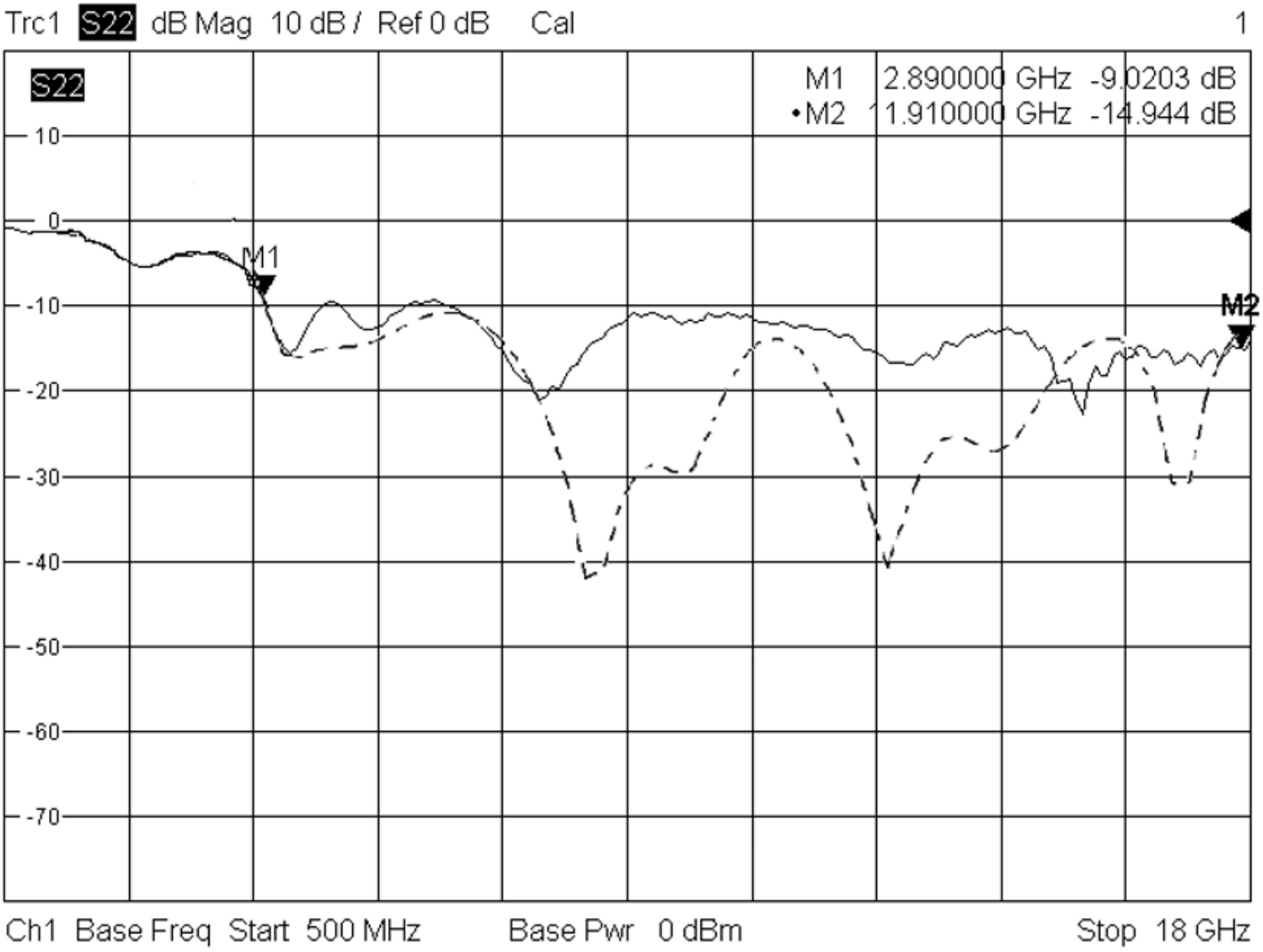

Figure 3

Impedance bandwidth of the proposed antenna.

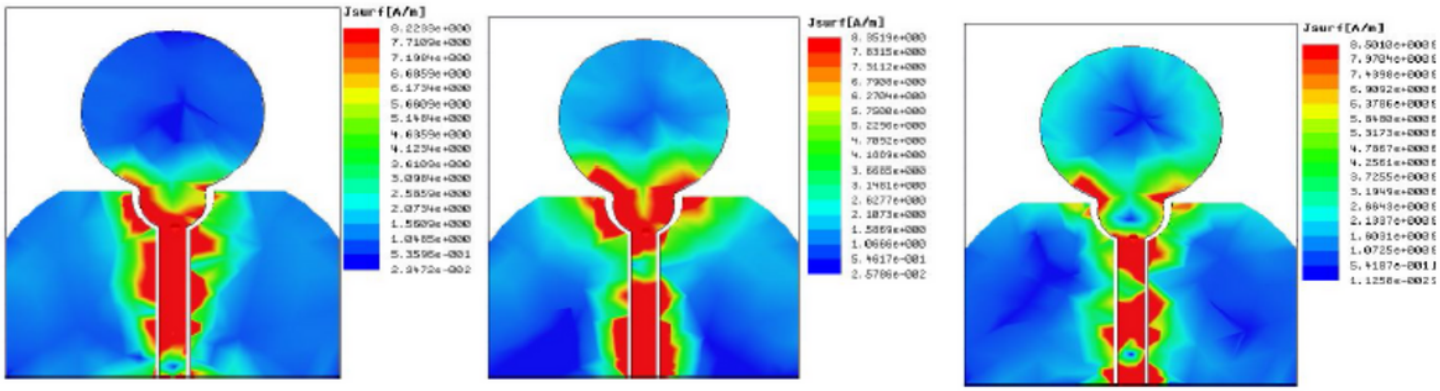

Figure 4

Current distribution of the guitar-shaped antenna at (a) 3.2 GHz, (b) 5.5 GHz, (c) 10 GHz.

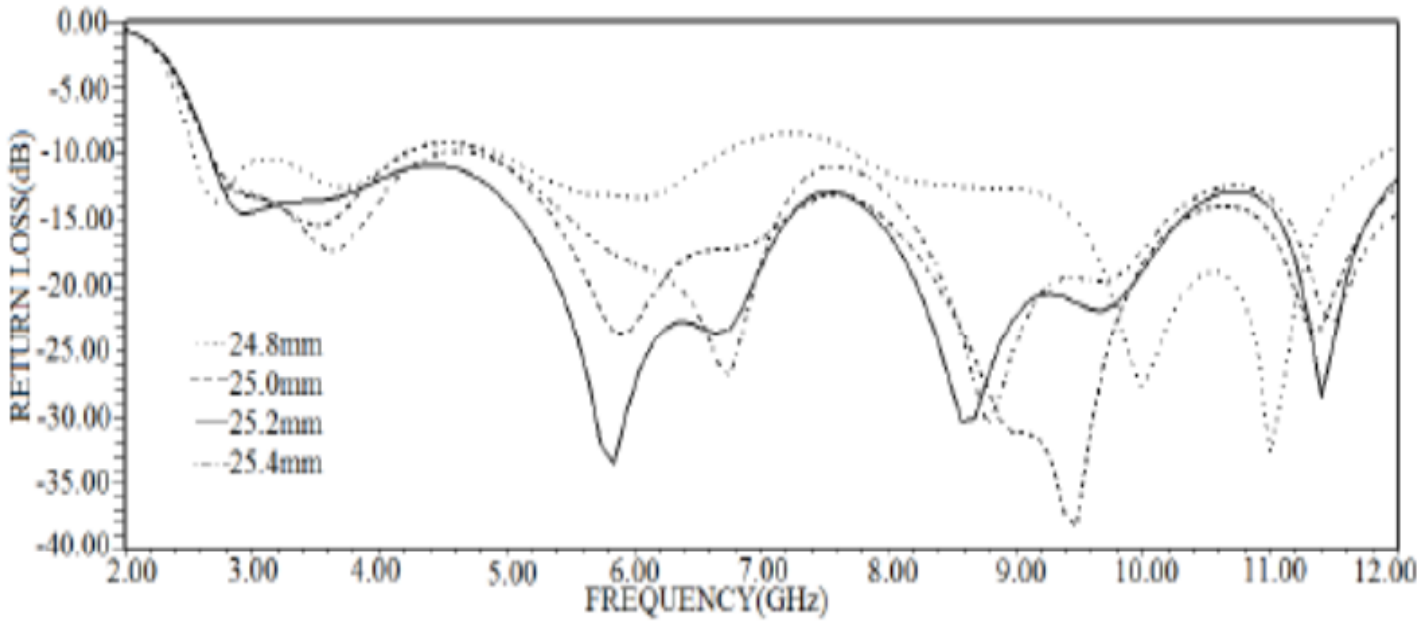

Figure 5

Optimization of the ground length.

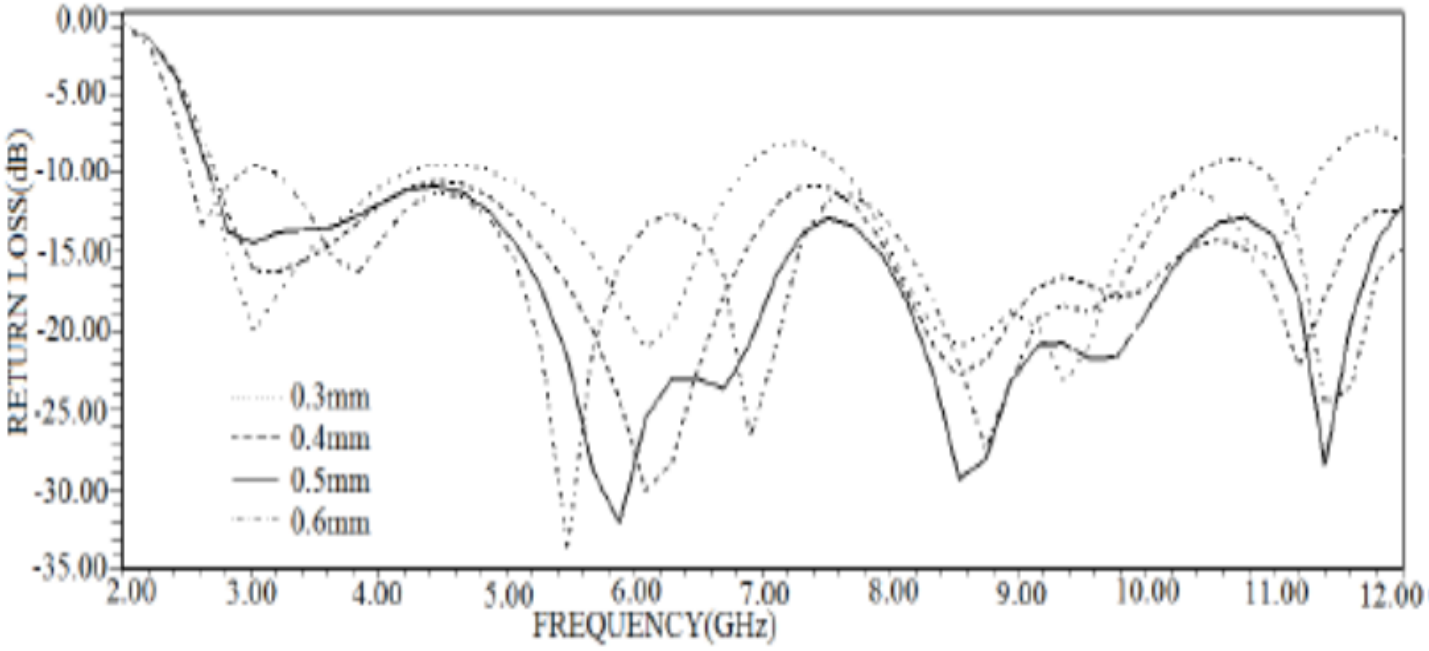

Figure 6

Optimization of the distance between ground and feedline.

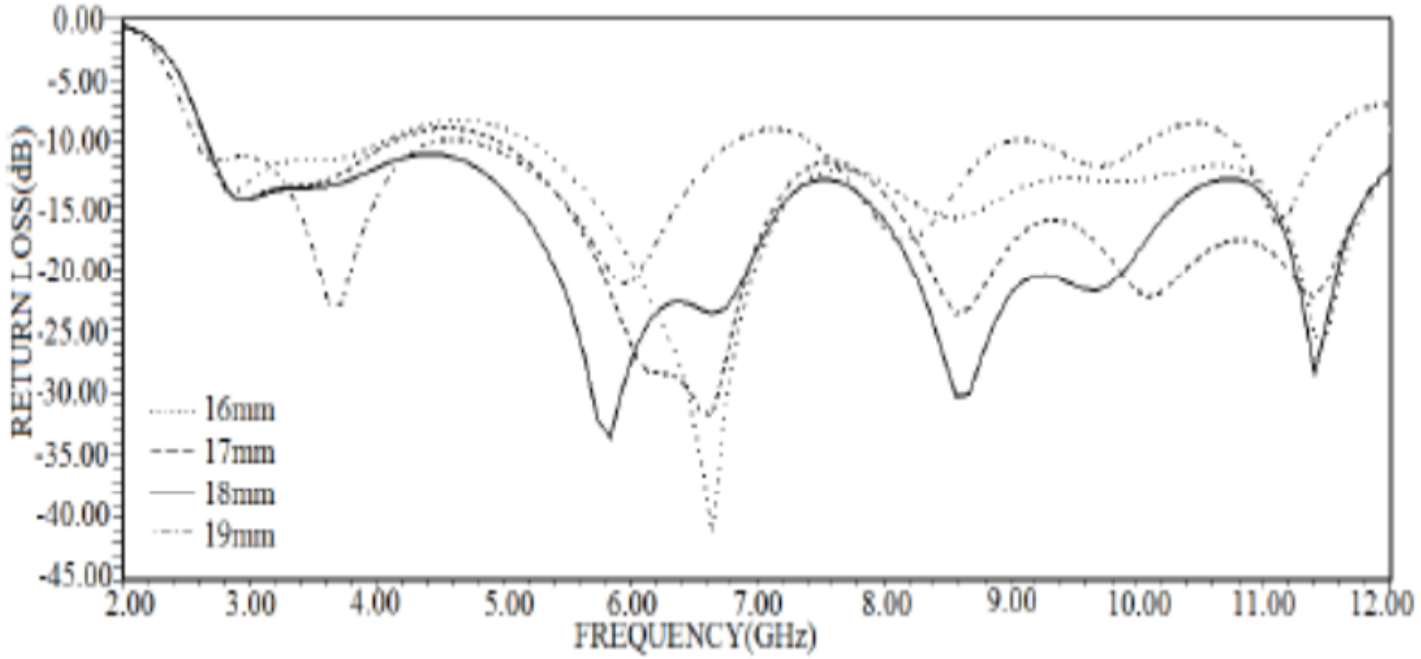

Figure 7

Optimization of ground curve at the edges.

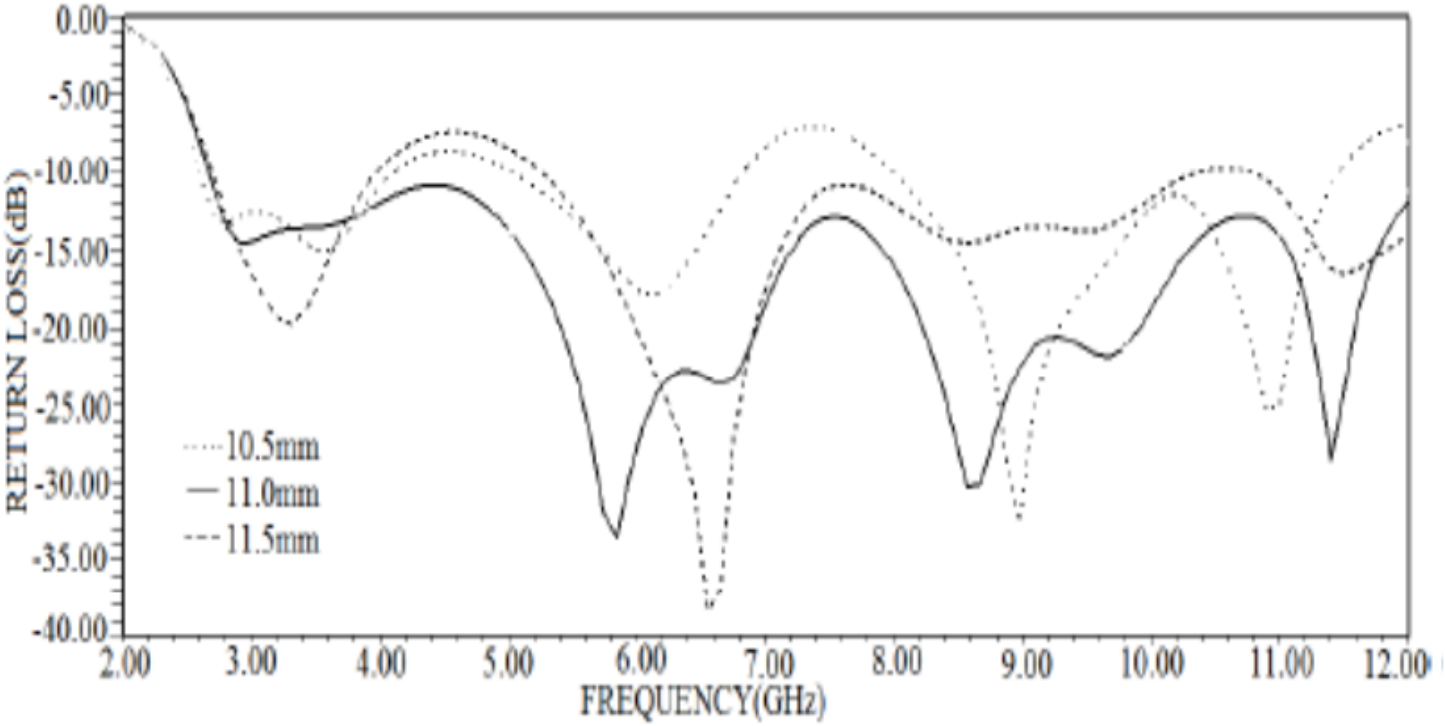

Figure 8

Optimization of the radius of the radiating patch.

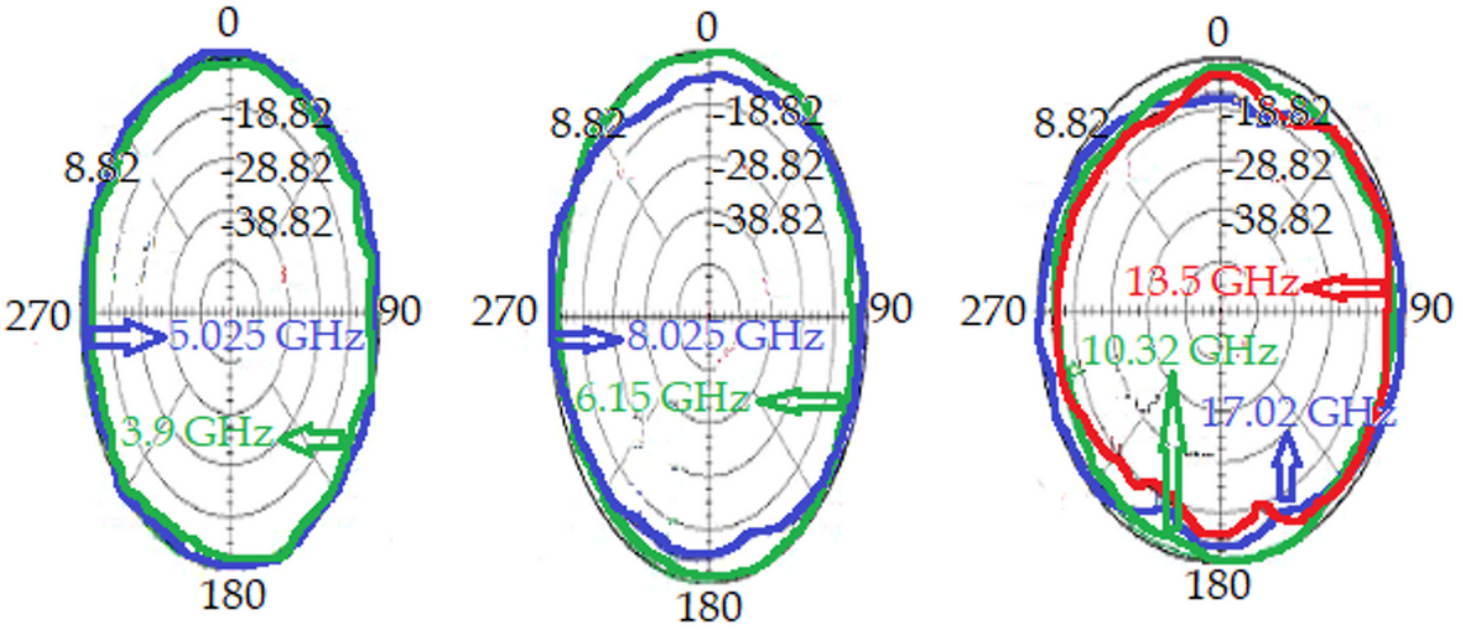

Figure 9

Measured H-plane radiation pattern of the antenna at (a) 3.9 GHz and 5.025 GHz, (b) 6.15 GHz and 8.025 GHz and (c) 10.32 GHz, 13.5 GHz and 17.02 GHz.

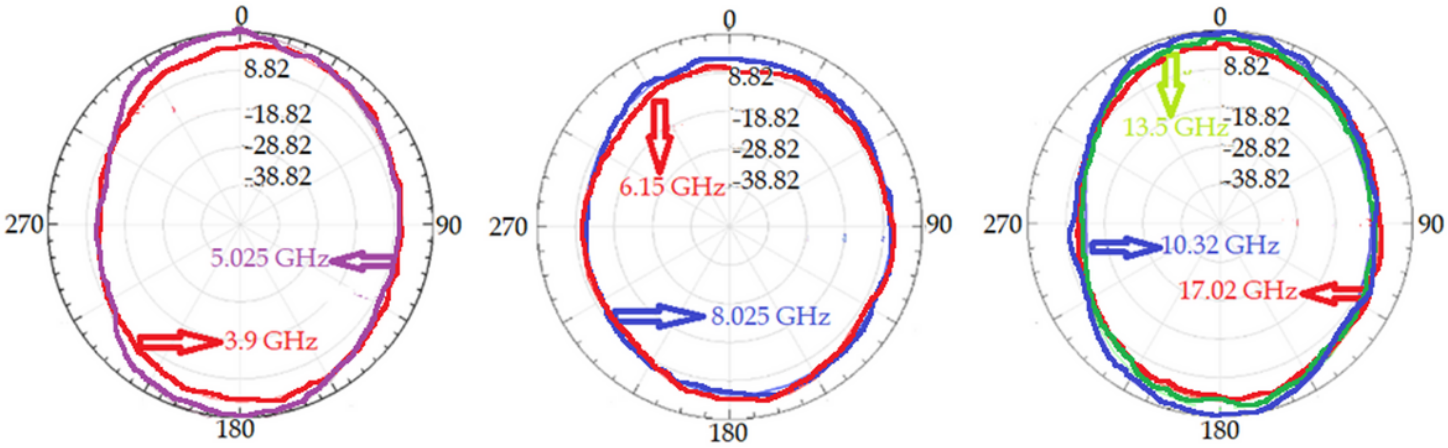

Figure 10

Simulated H-plane radiation pattern of the antenna at (a) 3.9 GHz and 5.025 GHz, (b) 6.15 GHz and 8.025 GHz and (c) 10.32 GHz, 13.5 GHz and 17.02 GHz.

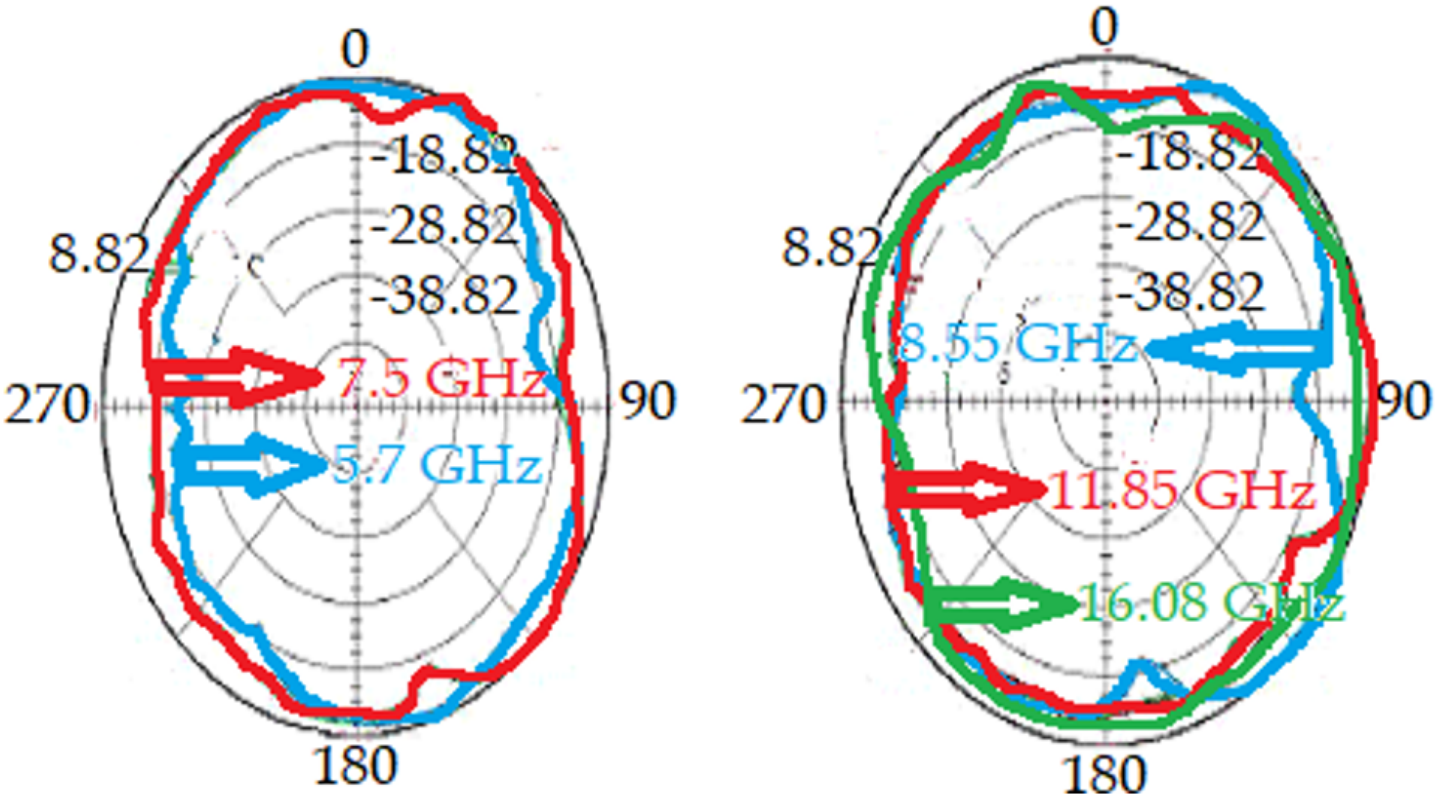

Figure 11

Measured E-plane radiation pattern of the antenna at (a) 5.7 GHz and 7.5 GHz and (b) 8.55 GHz, 11.85 GHz and 16.08 GHz.

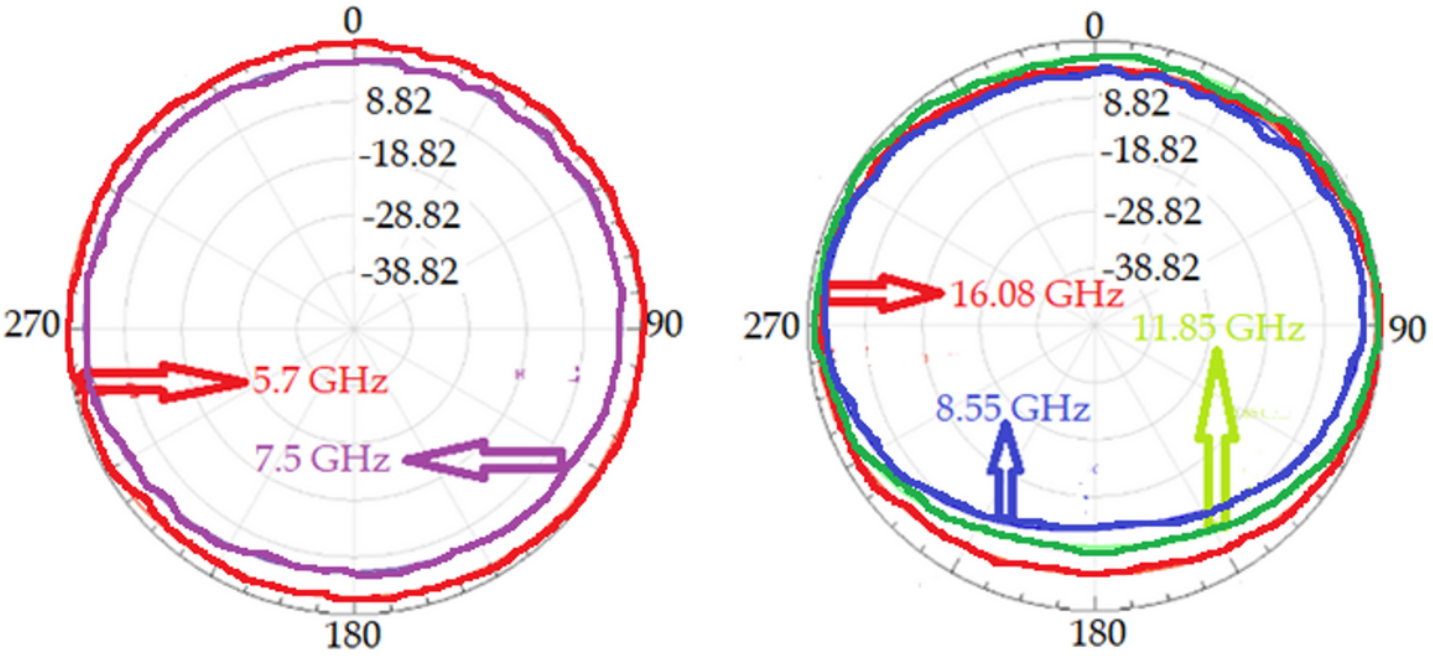

Figure 12

Simulated E-plane radiation pattern of the antenna at (a) 5.7 GHz and 7.5 GHz and (b) 8.55 GHz, 11.85 GHz and 16.08 GHz.

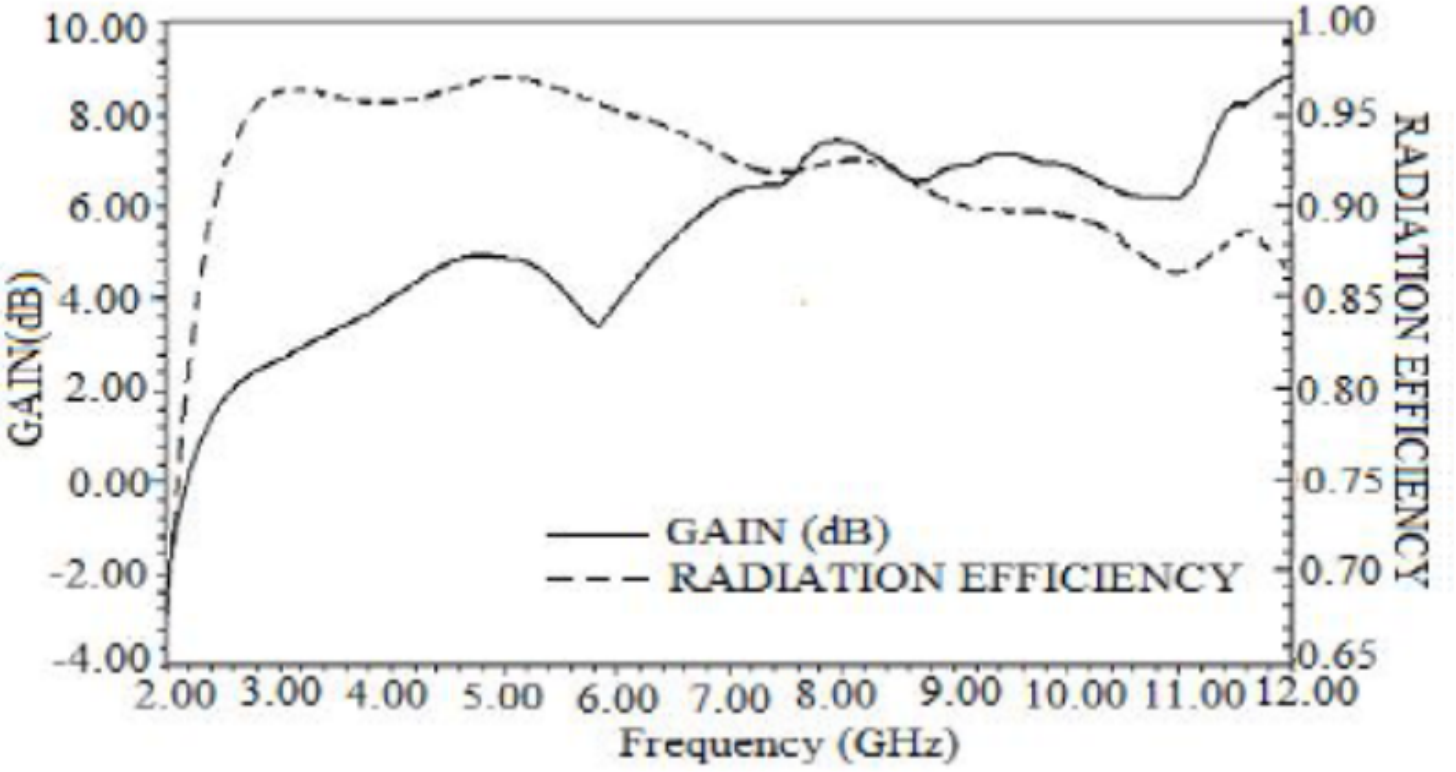

Figure 13

Simulated peak gain and radiation efficiency of the guitar-shaped antenna.